The 9th European Congress on Computational Methods in Applied Sciences and Engineering
ECCOMAS Congress 2024
3–7 June 2024, Lisboa, Portugal

TOPOLOGICAL DERIVATIVE-BASED HEAT SINK DESIGN WITH TEMPERATURE CONSTRAINTS

Giovanna C. Andrade[1], Antoine Laurain[2], Antonio A. Novotny[3]

[1] Instituto de Matemática e Estatística (IME), Universidade de São Paulo (USP)
R. do Matão, 1010, São Paulo - SP, 05508-090, Brazil,
email: gcandrade@ime.usp.br

[2] Fakultät für Mathematik, Universität Duisburg-Essen
Thea-Leymann-Str. 9, 45127 Essen, Germany
email: antoine.laurain@uni-due.de

[3] Laboratório Nacional de Computação Científica (LNCC/MCTI)
Coordenação de Métodos Matemáticos e Computacionais
Av. Getúlio Vargas 333, Petrópolis - RJ, 25651-075, Brazil,
email: novotny@lncc.br

Key words: Topology optimization, topological derivative, pointwise state constraints, temperature constraint, heat sink design

Summary. In this work we discuss a topological derivative-based strategy to address state-constrained problems in shape and topology optimization. Specifically, we investigate the design of optimal heat-sink structures under steady-state heat conduction and subject to temperature constraints. A quadratic penalty functional is formulated to realize the constraint and its first-order topological asymptotic expansion is derived. A difficulty that arises in the asymptotic analysis is exposed and handled using level-set representations of the subdomains in which the constraints are violated. The topology optimization problem is addressed with an efficient algorithm based on the topological derivative method, combined with a level set representation of the design domain, and numerical results are presented.

1 INTRODUCTION

State-constrained problems in shape and topology optimization arise in many practical applications. In heat transfer problems, for instance, temperature control is frequently important to avoid overheating of components or even unwanted phase transitions. In the context of additive manufacturing techniques, pointwise temperature constraints have been considered recently in path planning optimization for powder bed fusion [4], in casting process [8] and as an artificial strategy to impose connectivity constraints [7]. In the multi-physics setting, they have also been considered for the design of battery packs [5, 12]. In structural optimization, pointwise stress constraints are also important to avoid structural failure, although in this case the constraints are imposed on the gradient of the state, rather than directly on the state solution [1].

In general, realizing pointwise constraints is known to be a delicate issue. The strategy we adopt in this work is to formulate a quadratic penalty shape functional, so that the original optimization problem can be restated with a single equality constraint. Similar strategies have been considered in the shape sensitivity framework. In topological-derivative based methods, smooth penalty functionals have been introduced to mimic pointwise constraints on the gradient of the state [1]. Following a similar strategy, but in a multidimensional setting, Von Mises stress constraints in linear elasticity have been considered [3]. In such cases, the classical quadratic penalty is prohibited due to regularity issues (see [1, Remark 4.4]).

The main purpose of this work is to demonstrate that, in the specific case of constraints on the state, we can guarantee existence of the topological derivative of the quadratic penalty function. Then, we apply the topology design algorithm proposed by Amstutz and Andrä [2], which combines a level-set representation of the domain with the use of the topological derivative of the cost functional as a steepest-descent direction. The strategy is illustrated by a simple benchmark problem: the design of heat-sink structures under steady state heat conduction with temperature constraints.

This work is organized as follows. The problem statement is presented in Section 2. Then, the topological sensitivity analysis is discussed in Section 3 and the topological-derivative based algorithm is briefly described in Section 4. Finally, the methodology is illustrated by a simple benchmark problem in Section 5 and some concluding remarks and perspectives are given in Section 6.

2 PROBLEM STATEMENT

Let us consider a piecewise smooth, open and bounded set $\mathcal{D} \subset \mathbb{R}^2$ and define $\mathcal{P}(\mathcal{D})$ as a set of subsets of $\mathcal{D}$. For the present application, $\mathcal{D}$ represents a fixed domain which is split into two subdomains with different material properties: $\Omega \in \mathcal{P}(\mathcal{D})$ and its complement $\mathcal{D}\backslash\Omega$. We are interested in obtaining the optimal material distribution in the domain such that a certain shape functional $\mathcal{J}(\Omega)$, depending on the solution u_Ω of a partial differential equation (PDE), is minimized, while satisfying pointwise inequality constraints on u_Ω. Namely, we consider the following shape and topology optimization problem

$$\min_{\Omega\in\mathcal{P}(\mathcal{D})} \quad \mathcal{J}(\Omega), \quad \text{subject to} \quad u_\Omega(x) \leq u^*(x), \quad \forall x \in \Omega^*, \tag{1}$$

where Ω^* is a fixed subset of $\mathcal{D}$ in which the constraint is prescribed and u^* is a given positive function. In order to realize the pointwise constraint on the state, we define the following quadratic penalty functional

$$\mathcal{G}(\Omega) := \int_{\Omega^*} (u_\Omega - u^*)_+^2, \tag{2}$$

with $(u_\Omega - u^*)_+ := \max\{u_\Omega - u^*, 0\}$. With this choice, the constraint is satisfied almost everywhere in Ω^* if and only if $\mathcal{G}(\Omega) = 0$. Therefore, the optimization problem can be restated with a single equality constraint as

$$\min_{\Omega\in\mathcal{P}(\mathcal{D})} \quad \mathcal{J}(\Omega), \quad \text{subject to} \quad \mathcal{G}(\Omega) = 0. \tag{3}$$

In addition, we adopt a classical penalization scheme to impose the equality constraint, so that the final version of our optimization problem reads

$$\min_{\Omega\in\mathcal{P}(\mathcal{D})} \mathcal{L}(\Omega), \qquad \text{with} \qquad \mathcal{L}(\Omega) = \mathcal{J}(\Omega) + \Lambda^g \mathcal{G}(\Omega). \tag{4}$$

in which we introduce the positive parameter $\Lambda^g \to \infty$, see [9].

2.1 Heat-sink design formulation

As a model problem, we consider the design of an optimal heat-sink structure. The domain $\mathcal{D}$ is subjected to a heat source $q : \mathcal{D} \to \mathbb{R}$ and is assumed to be under steady state heat conduction. The fixed boundary $\partial\mathcal{D}$ is partitioned into two fixed subsets, Γ_n and Γ_d. A homogeneous Neumann boundary condition is imposed on Γ_n and a fixed temperature $\overline{u}$ is prescribed on the boundary Γ_d, which corresponds to a Dirichlet boundary condition, see Figure 1.

Let us define the function spaces $\mathcal{U} = \{v \in H^1(\mathcal{D}) : v = \overline{u} \text{ on } \Gamma_d\}$ and $\mathcal{V} = \{v \in H^1(\mathcal{D}) : v = 0 \text{ on } \Gamma_d\}$. Then, the state problem consists in the following two-phase Poisson problem with mixed boundary conditions

$$\text{Find} \quad u \in \mathcal{U} : \quad \int_{\mathcal{D}} \kappa \nabla u \cdot \nabla \varphi = \int_{\mathcal{D}} q\varphi, \qquad \forall \varphi \in \mathcal{V}, \tag{5}$$

in which u represents the domain's temperature and κ is the following piecewise constant function

$$\kappa = \kappa_\Omega \chi_\Omega + \kappa_{\mathcal{D}\setminus\Omega} \chi_{\mathcal{D}\setminus\Omega},$$

where κ_Ω and $\kappa_{\mathcal{D}\setminus\Omega}$ denote the thermal conductivities of phases Ω and $\mathcal{D}\setminus\Omega$, respectively, and χ_Ω, $\chi_{\mathcal{D}\setminus\Omega}$ are the characteristic functions associated to each subdomain. The boundary conditions and normal vector orientation are illustrated in Figure 1. For the optimization problem, we

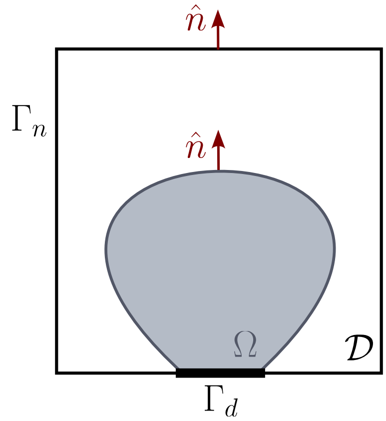

Figure 1: Representation of the domain $\mathcal{D}$ and its subset $\Omega \subset \mathcal{D}$, along with the problem's boundary conditions and normal vector orientation.

consider the minimization of the volume of phase Ω with a thermal compliance regularization term. Namely, we take

$$\mathcal{J}(\Omega) = V(\Omega) + \Lambda^c C(\Omega), \tag{6}$$

where Λ^c is a positive parameter and the volume and thermal compliance shape functionals are defined, respectively, as

$$V(\Omega) := \int_{\mathcal{D}} \chi_\Omega, \quad \text{and} \quad C(\Omega) := \int_{\mathcal{D}} qu. \tag{7}$$

In this formulation, the pointwise inequality constraint in (1) stands for a temperature constraint and the choice of Ω^* depends on the application.

3 TOPOLOGICAL SENSITIVITY ANALYSIS

The topological sensitivity analysis aims at studying the sensitivity of a given shape functional with respect to an infinitesimal singular perturbation of the geometry. For the current application, the topologically perturbed domain is obtained by nucleating a circular hole $B_\varepsilon(\hat{x})$. The hole produced by $B_\varepsilon(\hat{x})$ is then filled with a material distinct from the background. In particular, if the hole is nucleated in phase Ω, it is filled with a material corresponding to phase $\mathcal{D}\backslash\Omega$. Conversely, if it occurs in $\mathcal{D}\backslash\Omega$, then the converse is true. The thermal conductivity of

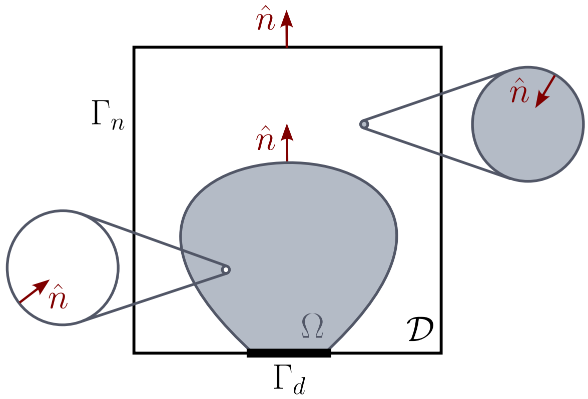

Figure 2: Representation of the topologically perturbed domain and normal vector orientation. Note that we take as a convention that the normal vector on $B_\varepsilon(\hat{x})$ is orientated towards the interior of the ball.

the perturbed domain is then characterized by the piecewise constant function $\kappa_\varepsilon := \gamma_\varepsilon \kappa$, with the *contrast* γ_ε defined as

$$\gamma_\varepsilon(x) := \begin{cases} 1 & \text{if } x \in \mathcal{D}\backslash B_\varepsilon(\hat{x}), \\ \gamma(x) & \text{if } x \in B_\varepsilon(\hat{x}), \end{cases} \qquad \text{with} \quad \gamma(x) := \begin{cases} (\kappa_{\mathcal{D}\backslash\Omega}/\kappa_\Omega) & \text{if } x \in \Omega, \\ (\kappa_{\mathcal{D}\backslash\Omega}/\kappa_\Omega)^{-1} & \text{if } x \in \mathcal{D}\backslash\Omega. \end{cases} \tag{8}$$

The variational formulation of the topologically perturbed state problem reads

$$u_\varepsilon \in \mathcal{U} : \quad \int_{\mathcal{D}} \kappa_\varepsilon \nabla u_\varepsilon \cdot \nabla \varphi = \int_{\mathcal{D}} q\varphi, \qquad \forall\, \varphi \in \mathcal{V}. \tag{9}$$

Note that, due to the inclusion, an interface condition holds on the border of B_ε. Also, the shape functionals $\mathcal{J}(\Omega_\varepsilon)$ and $\mathcal{G}(\Omega_\varepsilon)$ evaluated on the perturbed domain are expressed, respectively, as

$$\mathcal{J}(\Omega_\varepsilon) = \int_{\mathcal{D}} \chi_{\Omega_\varepsilon} + \Lambda^c \int_{\mathcal{D}} q u_\varepsilon. \tag{10}$$

and

$$\mathcal{G}(\Omega_\varepsilon) = \int_{\Omega^*} (u_\varepsilon - u^*)_+^2. \tag{11}$$

The topological sensitivity analysis of the volume and compliance shape functional is well known, see for instance [10]. Relying on these results and considering the linearity of the derivative operator, one obtains that the shape functional $\mathcal{J}(\Omega)$ admits the topological expansion

$$\mathcal{J}(\Omega_\varepsilon(\hat{x})) = \mathcal{J}(\Omega) + f(\varepsilon) D_T \mathcal{J}(\hat{x}) + o(\varepsilon^2), \tag{12}$$

with $f(\varepsilon) = \pi\varepsilon^2$ and the topological derivative

$$D_T\mathcal{J}(\hat{x}) = \alpha(\hat{x}) - 2\Lambda^c\frac{(1-\gamma)}{(1+\gamma)}\kappa\nabla u(\hat{x})\cdot\nabla v(\hat{x}), \tag{13}$$

in which $\alpha \coloneqq -\chi_\Omega + \chi_{\mathcal{D}\setminus\Omega}$ and v is the solution of the adjoint problem

$$v \in \mathcal{V} : \int_D \kappa\nabla v\cdot\nabla\varphi = -\int_{\mathcal{D}} q\varphi, \qquad \forall\, \varphi \in \mathcal{V}. \tag{14}$$

3.1 Topological derivative of the quadratic penalty shape functional

In this subsection, we seek for a topological expansion in the form of (12) for the shape functional $\mathcal{G}(\Omega)$. For a given function $\Phi \in H^1(\mathcal{D})$, we denote as ω_Φ the sublevel set $\omega_\Phi \coloneqq \{x \in \Omega^* : \Phi < 0\}$. Then, the subsets of Ω^* where the pointwise constraint on u and u_ε are violated are ω_ϕ and $\omega_{\phi_\varepsilon}$, with the auxiliary level-set functions

$$\phi \coloneqq -(u-u^*) \quad \text{and} \quad \phi_\varepsilon \coloneqq -(u_\varepsilon - u^*). \tag{15}$$

Based on such definitions, the variation of the cost function reads

$$\begin{aligned}\mathcal{G}(\Omega_\varepsilon) - \mathcal{G}(\Omega) &= \int_{\Omega^*}(u_\varepsilon - u^*)_+^2 - \int_{\Omega^*}(u-u^*)_+^2\\ &= \int_{\omega_{\phi_\varepsilon}}(u_\varepsilon - u^*)^2 - \int_{\omega_\phi}(u-u^*)^2.\end{aligned} \tag{16}$$

Next, we shall perform algebraic manipulations to collect the terms contributing to the topological derivative and residual norms. The main difficulty arising at this point is the dependence of $\omega_{\phi_\varepsilon}$ on ε. The impact of the perturbation on the active set ω_ϕ needs to be analyzed carefully using the asymptotic behavior of the solution u_ε with respect to the parameter. For this purpose, we can use the fact that ω_ϕ and $\omega_{\phi_\varepsilon}$ are level sets to compute an asymptotic expansion of (16), using results from [6]. Before discussing these ideas, let us first proceed with some manipulations in order to group terms which will be estimated in a similar manner. In fact, by summing and subtracting the terms

$$\int_{\omega_{\phi_\varepsilon}}(u-u^*)^2 \quad \text{and} \quad 2\int_{\Omega^*}(u_\varepsilon - u)(u-u^*)_+, \tag{17}$$

from (16), one obtains that $\mathcal{G}(\Omega_\varepsilon) - \mathcal{G}(\Omega) = I(\varepsilon) + \mathcal{E}_1(\varepsilon) + \mathcal{E}_2(\varepsilon)$ with

$$I(\varepsilon) \coloneqq 2\int_{\Omega^*}(u_\varepsilon - u)(u-u^*)_+, \tag{18}$$

$$\mathcal{E}_1(\varepsilon) \coloneqq \int_{\omega_{\phi_\varepsilon}}\phi(2h_\varepsilon + \phi) - \int_{\omega_\phi}\phi(2h_\varepsilon+\phi), \tag{19}$$

and

$$\mathcal{E}_2(\varepsilon) \coloneqq \int_{\omega_{\phi_\varepsilon}} h_\varepsilon^2, \tag{20}$$

in which we have introduced the notation $h_\varepsilon := \phi_\varepsilon - \phi$. Note that from definitions of the level set functions (15), we have that $h_\varepsilon = -(u_\varepsilon - u)$.

We will see that only the term I contributes to the topological derivative, whereas $\mathcal{E}_1$ and $\mathcal{E}_2$ are remainders. With this strategy, the issue of studying the behavior of the sets $\omega_{\phi_\varepsilon}$ and ω_ϕ is concentrated in term $\mathcal{E}_1$. The rest of the development is analogous to the one presented in [10, Chapter 3] for the compliance shape functional, for instance. Therefore, we describe the main ideas here and refer to [10] for more details.

Asymptotic behavior of the term $I(\varepsilon)$

In order to expand the term $I(\varepsilon)$ and extract its contribution to the topological derivative, we proceed as follows. Firstly, we introduce the adjoint state $p \in H^1(\mathcal{D})$, solution of the following variational problem

$$\text{Find } \ p \in \mathcal{V}: \quad \int_{\mathcal{D}} \kappa \nabla p \cdot \nabla \varphi = -2 \int_{\Omega^*} (u - u^*)_+ \varphi, \quad \forall\, \varphi \in \mathcal{V}. \tag{21}$$

Then, the weak formulations (5) and (9) of the original and perturbed state problems are used to express I as an integral defined over the ball B_ε. Namely,

$$I(\varepsilon) = -(1-\gamma) \int_{B_\varepsilon} \kappa \nabla u_\varepsilon \cdot \nabla p. \tag{22}$$

Next, we study the asymptotic behavior of the function u_ε with respect to the parameter ε by introducing the ansatz $u_\varepsilon(x) = u(x) + w_\varepsilon(x) + \tilde{u}_\varepsilon(x)$, where w_ε is the solution of

$$\begin{aligned} -\operatorname{div}(\kappa_\varepsilon \nabla w_\varepsilon) &= 0, && \text{in } \mathbb{R}^2, \\ w_\varepsilon &\to 0, && \text{for } |x| \to \infty, \\ [\![w_\varepsilon]\!] &= 0, && \text{on } \partial B_\varepsilon(\hat{x}), \\ [\![\kappa_\varepsilon \nabla w_\varepsilon]\!] \cdot n &= \hat{v}, && \text{on } \partial B_\varepsilon(\hat{x}), \end{aligned} \tag{$\mathcal{P}_{w_\varepsilon}$}$$

with $\hat{v} = -(1-\gamma)(\kappa \nabla u(\hat{x})) \cdot n$, and $\tilde{u}_\varepsilon$ is the solution of

$$\begin{aligned} -\operatorname{div}(\kappa_\varepsilon \nabla \tilde{u}_\varepsilon) &= -(1-\gamma) \operatorname{div}(\kappa \nabla u)_{|B_\varepsilon}, && \text{in } \mathcal{D}, \\ \tilde{u}_\varepsilon &= -w_\varepsilon, && \text{on } \Gamma_d, \\ (\kappa_\varepsilon \nabla \tilde{u}_\varepsilon) \cdot n &= -(\kappa \nabla w_\varepsilon) \cdot n, && \text{on } \Gamma_n, \\ [\![\tilde{u}_\varepsilon]\!] &= 0, && \text{on } \partial B_\varepsilon(\hat{x}), \\ [\![\kappa_\varepsilon \nabla \tilde{u}_\varepsilon]\!] \cdot n &= -(1-\gamma) \left[(\kappa \nabla u) \cdot n - (\kappa \nabla u(\hat{x})) \cdot n \right], && \text{on } \partial B_\varepsilon(\hat{x}). \end{aligned} \tag{$\mathcal{P}_{\tilde{u}_\varepsilon}$}$$

Further, we can prove that ($\mathcal{P}_{w_\varepsilon}$) admits the explicit unique solution

$$w_\varepsilon(x)_{|B_\varepsilon} = \frac{(1-\gamma)}{(1+\gamma)} \nabla u(\hat{x}) \cdot (x - \hat{x}), \tag{23}$$

$$w_\varepsilon(x)_{|\mathbb{R}^2 \setminus B_\varepsilon} = \frac{(1-\gamma)}{(1+\gamma)} \frac{\varepsilon^2}{\|x - \hat{x}\|} \nabla u(\hat{x}) \cdot (x - \hat{x}), \tag{24}$$

so that, by replacing the ansatz for u_ε in (22), we obtain

$$\mathcal{G}(\Omega_\varepsilon) - \mathcal{G}(\Omega) = -2\frac{(1-\gamma)}{(1+\gamma)}\kappa\nabla u(\hat{x})\cdot\nabla p(\hat{x})\pi\varepsilon^2 + \sum_{i=1}^{5}\mathcal{E}_i(\varepsilon), \tag{25}$$

with the additional remainders

$$\mathcal{E}_3(\varepsilon) = -(1-\gamma)\int_{B_\varepsilon}\kappa\nabla\tilde{u}_\varepsilon\cdot\nabla p, \tag{26}$$

$$\mathcal{E}_4(\varepsilon) = -(1-\gamma)\int_{B_\varepsilon}\kappa\nabla w_\varepsilon\cdot(\nabla p - \nabla p(\hat{x})), \tag{27}$$

and

$$\mathcal{E}_5(\varepsilon) = -(1-\gamma)\int_{B_\varepsilon}\kappa\left[\nabla u\cdot\nabla p - \nabla u(\hat{x})\cdot\nabla p(\hat{x})\right]. \tag{28}$$

Asymptotic behavior of the remainders $\mathcal{E}_i(\varepsilon)$, for $i = 2,\dots 5$

Note that the estimates $\|u_\varepsilon - u\|_{H^1(\mathcal{D})} \approx \varepsilon$ and $\|\tilde{u}_\varepsilon\|_{H^1(\mathcal{D})} \approx \varepsilon^2$ hold true (see [10, Lemma 3.1 and Lemma 3.2] for a complete proof of analogous estimates for a similar problem, with an additional first order term in the PDE). Then, considering the explicit expression (23) of w_ε inside B_ε and the interior elliptic regularity of u and p, we obtain that the remainders $\mathcal{E}_3$, $\mathcal{E}_4$ and $\mathcal{E}_5$ are of order $o(\varepsilon^2)$, see [10, Section 3.4]. For term $\mathcal{E}_2$, defined in (20), observe that

$$|\mathcal{E}_2(\varepsilon)| = \|h_\varepsilon\|^2_{L^2(w_{\phi_\varepsilon})} \leq \|h_\varepsilon\|^2_{L^2(\mathcal{D})}. \tag{29}$$

An estimate for h_ε in $L^2(\mathcal{D})$ can be obtained based on the ansatz proposed for u_ε. In fact, based on the explicit expression for w_ε, given by (23) and (24), one can show that $\|w_\varepsilon\|_{L^2(\mathcal{D})} \approx \varepsilon^2\sqrt{\ln|\varepsilon|}$ (see [10, Chapter 3]), so that

$$\|h_\varepsilon\|_{L^2(\mathcal{D})} \approx \varepsilon^2\sqrt{\ln|\varepsilon|}. \tag{30}$$

Thus, we obtain that the remainder $\mathcal{E}_2$ is of order $o(\varepsilon^3)$.

Asymptotic behavior of the remainder $\mathcal{E}_1(\varepsilon)$

Finally, we study the more involved case of $\mathcal{E}_1$. First, let us notice that this term can be restated as $\mathcal{E}_1(\varepsilon) = \mathcal{F}(\omega_{\phi_\varepsilon}) - \mathcal{F}(\omega_\phi)$ introducing the shape functional

$$\mathcal{F}(\omega) \coloneqq \int_\omega \phi(2h_\varepsilon + \phi). \tag{31}$$

In order to prove that this term is a remainder, we will verify that $\mathcal{E}_1$ can be expressed in terms of the shape derivative of $\mathcal{F}$. Recall that, for a given vector field $\theta \in C^\infty(\mathcal{D}, \mathbb{R}^d)$ and its associated flow $T_t^\theta : \overline{\mathcal{D}} \to \mathbb{R}^d$, $t \in [0,\tau]$, the shape derivative of $\mathcal{F}$ at a certain set $\omega \subset \mathcal{D}$ in direction θ is given by

$$d\mathcal{F}(\omega)(\theta) \coloneqq \lim_{t\searrow 0}\frac{\mathcal{F}(\omega_t) - \mathcal{F}(\omega)}{t}, \tag{32}$$

where $\omega_t \coloneqq T_t^\theta(\omega)$ is a perturbation of ω, see for instance [11]. Next, we introduce the family of parameterized level set functions $\phi_s \coloneqq \phi + sh_\varepsilon$, for $s \in [0,1]$, and the associated sublevel set ω_{ϕ_s}. Then, we have the following lemma.

Lemma 1. *For each $s \in [0,1]$, assume that ω_{ϕ_s} is sufficiently smooth with $\partial\omega_{\phi_s} \cap \partial\Omega^* = \emptyset$ and $|\nabla\phi_s| > 0$ on $\partial\omega_{\phi_s}$. Then,*

$$\mathcal{E}_1(\varepsilon) = \int_0^1 d\mathcal{F}(\omega_{\phi_s})(\theta_s)ds = \int_0^1 \left[\int_{\partial\omega_{\phi_s}} \phi(2h_\varepsilon + \phi)\theta_s \cdot n_s\right] ds, \tag{33}$$

where $\theta_s := -h_\varepsilon|\nabla\phi_s|^{-2}\nabla\phi_s$ on $\partial\omega_{\phi_s}$ and n_s is the outward unit normal vector to ω_{ϕ_s}.

Proof. For a fixed $s \in [0,1]$ the functional $\mathcal{F}$ is shape differentiable at ω_{ϕ_s}. Furthermore, for a given vector field $\theta \in C^\infty(\mathcal{D}, \mathbb{R}^d)$, the shape derivative is given by

$$d\mathcal{F}(\omega_{\phi_s})(\theta) = \int_{\partial\omega_{\phi_s}} \phi(2h_\varepsilon + \phi)\theta \cdot n_s, \tag{34}$$

in which n_s is the outward unit vector to ω_{ϕ_s}, see for instance [11]. Next, let us introduce the functional $F(\Phi) := \mathcal{F}(\omega_\Phi)$, for $\Phi \in H^1(\mathcal{D})$. With this definition, note that $\mathcal{E}_1 = F(\phi_\varepsilon) - F(\phi)$. Then, it follows from [6, Theorem 3] that we can establish a link between the shape derivative of $\mathcal{F}$ and the Gâteaux derivative of F. Namely, we obtain that the application F is Gâteaux differentiable at ϕ_s and

$$d_G F(\phi_s)(h_\varepsilon) = d\mathcal{F}(\omega_{\phi_s})(\theta_s), \tag{35}$$

where $d_G F(\phi_s)(h_\varepsilon)$ denotes the Gâteaux derivative at ϕ_s in direction h_ε, and

$$\theta_s := -h_\varepsilon|\nabla\phi_s|^{-2}\nabla\phi_s \quad \text{on} \quad \partial\omega_{\phi_s}. \tag{36}$$

Now, let $\eta : [0,1] \to \mathbb{R}$ be the map $\eta(s) := F(\phi_s) = F(\phi + sh_\varepsilon)$. Then, it follows from the chain rule that η is differentiable at each $s \in [0,1]$ and

$$\eta'(s) = \frac{d}{ds}F(\phi_s) = d_G F(\phi_s)(h_\varepsilon). \tag{37}$$

Also, note that η is absolutely continuous and that the application $[0,1] \ni s \mapsto d_G F(\phi_s)(h_\varepsilon)$ belongs to $L^1(0,1)$. Therefore, it follows from the Fundamental Theorem of Calculus that

$$\mathcal{E}_1(\varepsilon) \overset{(37)}{=} \int_0^1 d_G F(\phi_s)(h_\varepsilon)ds \overset{(35)}{=} \int_0^1 d\mathcal{F}(\omega_{\phi_s})(\theta_s)ds. \tag{38}$$

Then, considering the expression of the shape derivative (34), we obtain the desired result. □

Note that the previous result is only possible because ω_ε and ω have level-set representations, which allow the definition of the functional F, defined on usual vector spaces. Next, based on expression (33), we estimate $\mathcal{E}_1$. In fact, note that

$$\mathcal{E}_1(\varepsilon) = \int_0^1 \underbrace{\left[\int_{\partial\omega_{\phi_s}} \phi_s(2h_\varepsilon + \phi)\theta_s \cdot n_s\right]}_{=0} ds + \int_0^1 s \underbrace{\left[\int_{\partial\omega_{\phi_s}} (-h_\varepsilon)(2h_\varepsilon + \phi)\theta_s \cdot n_s\right]}_{=:L} ds, \tag{39}$$

where we have used the fact that $\phi_s = 0$ on $\partial\omega_{\phi_s}$ by definition. Now let us study the term L. Considering the definition (36) of θ_s and $n_s = \nabla\phi_s|\nabla\phi_s|^{-1}$, we have that

$$L = \int_{\partial\omega_{\phi_s}} \frac{h_\varepsilon^2(2h_\varepsilon + \phi)}{|\nabla\phi_s|}. \tag{40}$$

Next, we assume that there exist constants c_1 and c_2, independent of s and ε, such that $|\nabla\phi_s| > c_1$ and $\|2h_\varepsilon + \phi\|_{L^\infty(\partial\omega_{\phi_s})} < c_2$. Then, if follows from (40) that $|L| \leq C\|h_\varepsilon\|^2_{L^2(\partial\omega_{\phi_s})}$. Furthermore, this norm can be bounded by the estimate of h_ε in $L^2(\mathcal{D})$, obtained in (30). Hence, we obtain

$$|\mathcal{E}_1(\varepsilon)| \leq \int_0^1 s\frac{c_2}{c_1}\varepsilon^4 \ln|\varepsilon| ds \leq \frac{1}{2}\frac{c_2}{c_1}\varepsilon^4 \ln|\varepsilon|, \tag{41}$$

which means that $\mathcal{E}_1$ is of order $o(\varepsilon^3)$. Thus, we have obtained the following result.

Theorem 1. *The quadratic penalty functional* (2) *admits the following first-order topological asymptotic expansion*

$$\mathcal{G}(\Omega_\varepsilon(\hat{x})) = \mathcal{G}(\Omega) + f(\varepsilon)D_T\mathcal{G}(\hat{x}) + o(\varepsilon^2),$$

with $f(\varepsilon) = \pi\varepsilon^2$ *and*

$$D_T\mathcal{G}(\hat{x}) = -2\frac{(1-\gamma)}{(1+\gamma)}\kappa\nabla u(\hat{x}) \cdot \nabla p(\hat{x}),$$

in which p is the solution of the following adjoint problem

$$\textit{Find}\ \ p \in \mathcal{V}: \quad \int_{\mathcal{D}} \kappa\nabla p \cdot \nabla\varphi = -2\int_{\Omega^*} (u - u^*)_+\varphi, \quad \forall\ \varphi \in \mathcal{V}. \tag{42}$$

4 TOPOLOGY DESIGN ALGORITHM

The topological-derivative based algorithm we employ here was initially proposed by Amstutz and Andrä [2] and designed specifically to work with domains perturbed by ball-shaped inclusions, such as the ones described in the previous section. The domain $\mathcal{D}$ is fixed and the subdomain Ω is represented as the negative sublevel set of an auxiliary function $\Psi : \mathcal{D} \to \mathbb{R}$. For each iteration n, the algorithm basically consists in the following steps. First, we identify the domain Ω_n implicitly described by the level set function Ψ_n. Then, the corresponding state problem and the cost functionals are evaluated. Next, the topological derivative of the cost functional is computed and is used as a steepest descent direction to update the level set function Ψ_n. If this step decreases the cost function, then it is accepted, otherwise we perform a line search. If the step size becomes too small, a mesh refinement is tried, whereas if the stopping criteria is satisfied, then the algorithm is interrupted. The seeked criteria in this algorithm is a local sufficient optimality condition, which, for the class of perturbations under consideration, can be stated as $D_T\mathcal{L}(\hat{x}) > 0$, for all $\hat{x} \in \mathcal{D}$. For more details, see [2].

5 NUMERICAL EXPERIMENTS

Let us consider a square domain $\mathcal{D} = [0,1] \times [0,1]$ subject to a unit heat source and with a Dirichlet boundary condition prescribed in the central portion of the bottom boundary with length $|\Gamma_d| = 0.2$. Also, we take $\Omega^* = \mathcal{D}$ in (2), which means that the temperature value is constrained on both phases of the domain. The thermal conductivity of phase Ω is set as $\kappa = 1.0$, whereas for phase $\mathcal{D}\backslash\Omega$ we experiment with three different values $\kappa_{\mathcal{D}\backslash\Omega} = 0.5$, $\kappa_{\mathcal{D}\backslash\Omega} = 0.1$ and $\kappa_{\mathcal{D}\backslash\Omega} = 0.05$. For numerical purposes, the volume and compliance have been normalized by the corresponding shape functionals evaluated on the initial domain. For the thermal compliance regularization term we set $\Lambda^j = 0.4$, whereas the penalty factor of the temperature constraint shape functional is fixed as $\Lambda^g = 9 \times 10^3$. Indeed, from a mathematical point of view, problems (3) and (4) are equivalent only when $\Lambda^g \to \infty$. Therefore, it was chosen based on preliminary experiments as the largest possible value for which numerical errors did not appear.

Let us first observe that Ω is the phase filled with the best conductor, so that $\Omega = \mathcal{D}$ (full domain) is the case which best conducts heat. Therefore, if u^* is set as any value lower than the maximum temperature reached in this case, then the constraint $u(x) \leq u^*(x)$ in (1) will certainly be violated. On the other hand, the unconstrained problem gives an idea of an upper bound for the choice of u^* in order for it to actually have an effect on the optimal design. In Table 1, we exhibit the solution of the state equation in the full domain and the unconstrained optimal designs obtained with three different choices of $\kappa_{\mathcal{D}\backslash\Omega}$. Based on these considerations, we choose for the present benchmark problem three different values of u^*, namely $u^* = 1.0$, $u^* = 1.2$ and $u^* = 1.4$.

Table 1: Solution of the state equation in the full domain ($\Omega = \mathcal{D}$), and in the unconstrained optimal designs obtained with different values of $\kappa_{\mathcal{D}\backslash\Omega}$. The optimal designs and the temperature field are presented together in the same figure.

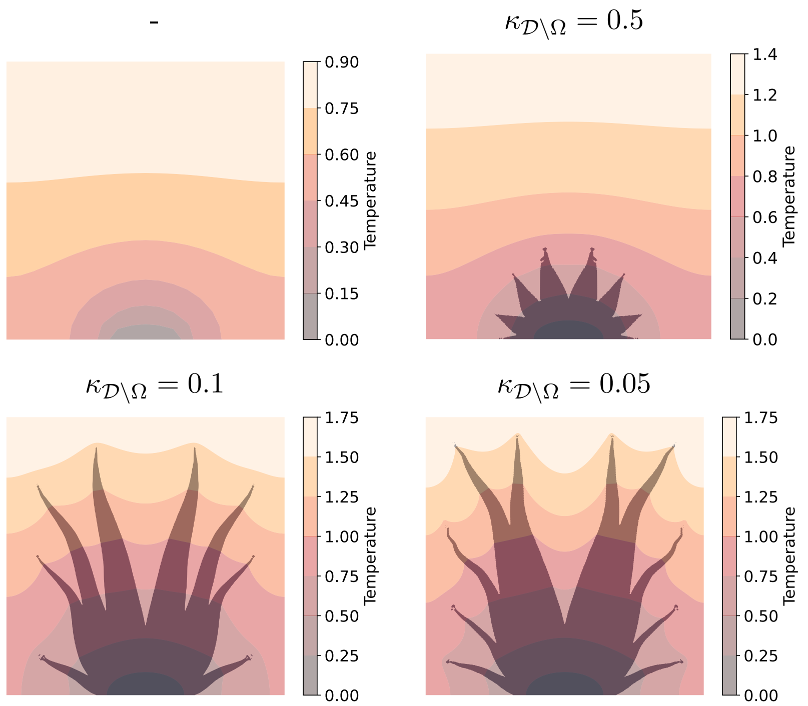

In Table 2, the optimal designs obtained with different choices of u^* and $\kappa_{\mathcal{D}\backslash\Omega}$ are presented. The yellow region indicates the portion of the domain for which the temperature constraint is violated. In the worst case obtained, it corresponds to 3.34% of the domain. For a fixed value of $\kappa_{\mathcal{D}\setminus\Omega}$, we observe that when a smaller value of u^* is chosen, the volume of phase Ω increases, which is consistent with the fact that more conductive material is needed in order to dissipate the heat and satisfy the constraint. The area of the region in which the constraint is violated also increases as u^* decreases, indicating that the constraint becomes more difficult to satisfy. On the other hand, as the value of $\kappa_{\mathcal{D}\setminus\Omega}$ decreases, it is interesting to observe that not only the volume of phase Ω increases, but the design also tends to become more spread in the domain. Indeed, as we decrease $\kappa_{\mathcal{D}\setminus\Omega}$, phase Ω increasingly becomes the primary conductor of heat, making its presence essential for extracting heat from the extremities of the domain.

Table 2: Optimal designs obtained with different values of $\kappa_{\mathcal{D}\setminus\Omega}$ and u^*.

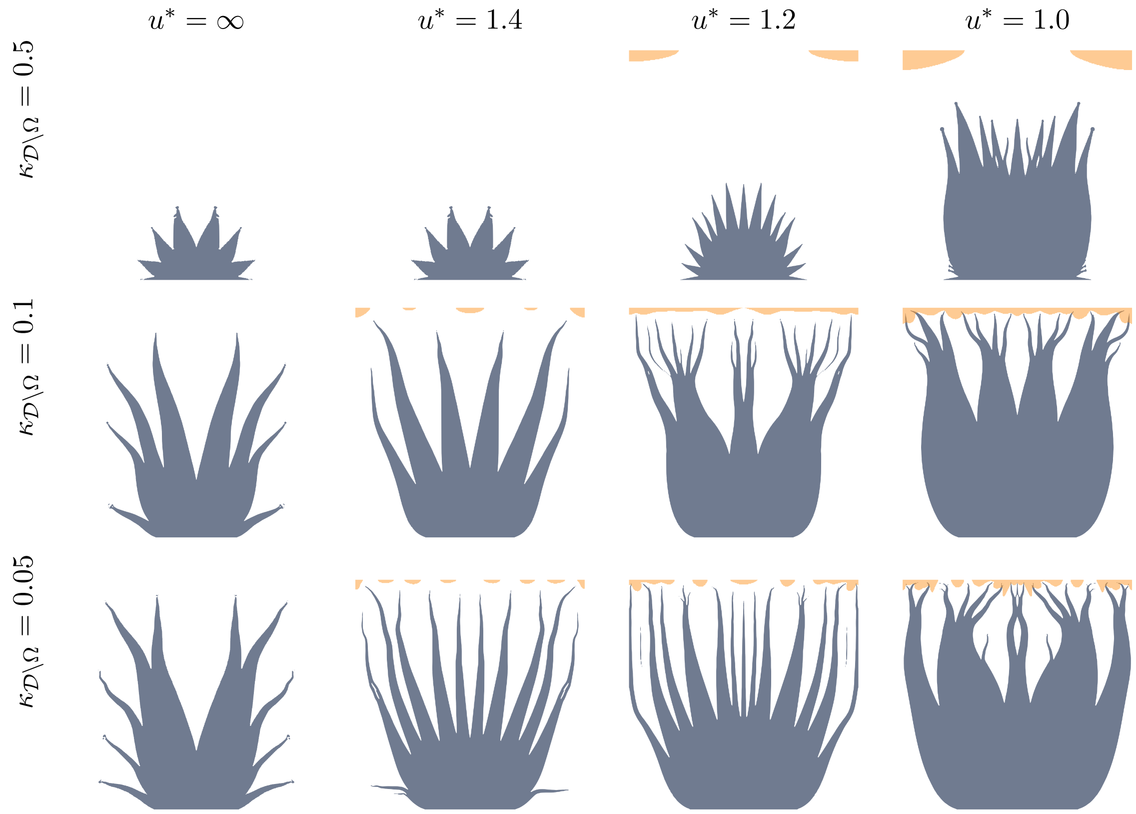

6 CONCLUSIONS AND PERSPECTIVES

We have investigated a simple quadratic penalty formulation to realize pointwise constraints in the solution of the state problem, in the framework of topological-derivative based methods. Specifically, we have shown existence of the topological derivative in a continuous setting. Numerical experiments have confirmed the expected trade-off between the optimal domain's volume and the temperature constraint, revealing the need of allocating more conductive material as tighter constraints are imposed. For future works, we will apply the same strategy to more complex problems, such as problems posed in a multi-physics setting. Additionally, we will study the case $\Omega^* = \Omega$, i.e., when the constraint is imposed on only one phase of the domain.

7 ACKNOWLEDGEMENTS

The present work was supported by FAPESP, Grant 2021/14604-1.

REFERENCES

[1] S. Amstutz. A penalty method for topology optimization subject to a pointwise state constraint. *ESAIM: Control, Optimisation and Calculus of Variations*, 16(3):523–544, 2010.

[2] S. Amstutz and H. Andrä. A new algorithm for topology optimization using a level-set method. *Journal of Computational Physics*, 216(2):573–588, 2006.

[3] S. Amstutz and A. A. Novotny. Topological optimization of structures subject to von Mises stress constraints. *Structural and Multidisciplinary Optimization*, 41(3):407–420, 2010.

[4] M. Boissier. *Coupling structural optimization and trajectory optimization methods in additive manufacturing*. Theses, Institut Polytechnique de Paris, 2020.

[5] S. Kambampati, J. S. Gray, and H. A. Kim. Level set topology optimization of structures under stress and temperature constraints. *Computers & Structures*, 235:106265, 2020.

[6] A. Laurain. Analyzing Smooth and Singular Domain Perturbations in Level Set Methods. *SIAM Journal on Mathematical Analysis*, 50(4):4327–4370, 2018.

[7] P. Li, Y. Wang, Z. Wang, and Y. Zhaoi. Inverse obstacle scattering for elastic waves. *Inverse Problems*, 32:115018, 2016.

[8] G. Michailidis. *Manufacturing Constraints and Multi-Phase Shape and Topology Optimization via a Level-Set Method*. PhD Thesis, 2014.

[9] J. Nocedal and S. Wright. *Numerical Optimization*. Springer Series in Operations Research and Financial Engineering. Springer New York, 2006.

[10] A. A. Novotny and J. Sokołowski. *An introduction to the topological derivative method*. Springer Briefs in Mathematics. Springer Nature Switzerland, 2020.

[11] J. Sokołowski and J. P. Zolésio. *Introduction to Shape Optimization: Shape Sensitivity Analysis*. Springer-Verlag, Berlin, Germany, 1992.

[12] X. Zhu, C. Zhao, X. Wang, Y. Zhou, P. Hu, and Z.-D. Ma. Temperature-constrained topology optimization of thermo-mechanical coupled problems. *Engineering Optimization*, 51(10):1687–1709, 2019. Publisher: Taylor & Francis.